Supporting information

Insights into (Mn/Fe/Co)M-N-C Dual-Atom Catalysts for the Oxygen Reduction Reaction: The Critical Role of Structural Evolution

Xiaoming Zhang[a,b,c], Suli Wang[a,c]*, Zhangxun Xia[a,c], Huanqiao Li[a,c], Shansheng Yu[d] and Gongquan Sun[a,c]*

[1]Division of Fuel Cells and Battery, Dalian National Laboratory for Clean Energy, Dalian Institute of Chemical Physics, Chinese Academy of Sciences, Dalian 116023, China

[2]Center of Materials Science and Optoelectronics Engineering, University of Chinese Academy of Sciences, Beijing 100049, China

[3]Key Laboratory of Fuel Cells & Hybrid Power Sources, Chinese Academy of Sciences, Dalian 116023, China

[4]Department of Materials Science, Jilin University, Changchun 130012, China

Keywords: diatomic catalyst, DFT, ORR, activity and stability

*Corresponding author: Suli Wang, e-mail: suliwang@dicp.ac.cn & Gongquan Sun, e-mail: gqsun@dicp.ac.cn

Figures and Tables

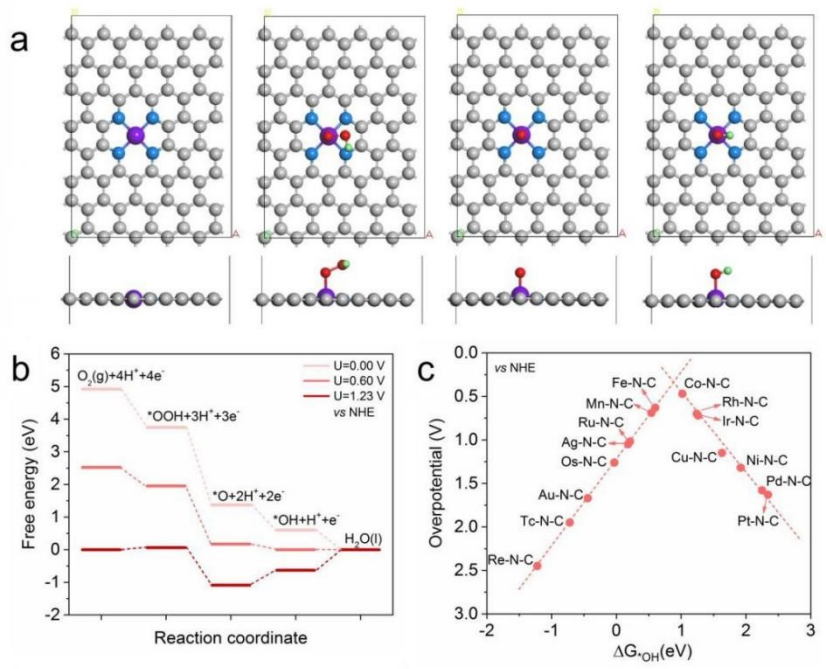

Figure S 1. (a) The optimized geometry structures of Fe-N-C, *OOH-Fe-N-C, *O-Fe-N-C,and *OH-Fe-N-C. (b) The ORR free energy diagram of Fe-N-C. (c) The volcano plot between overpotential and ΔG_{*OH} of M-N-C. Gray: C; Purple: Fe; Blue: N; Red: O; Green: H.

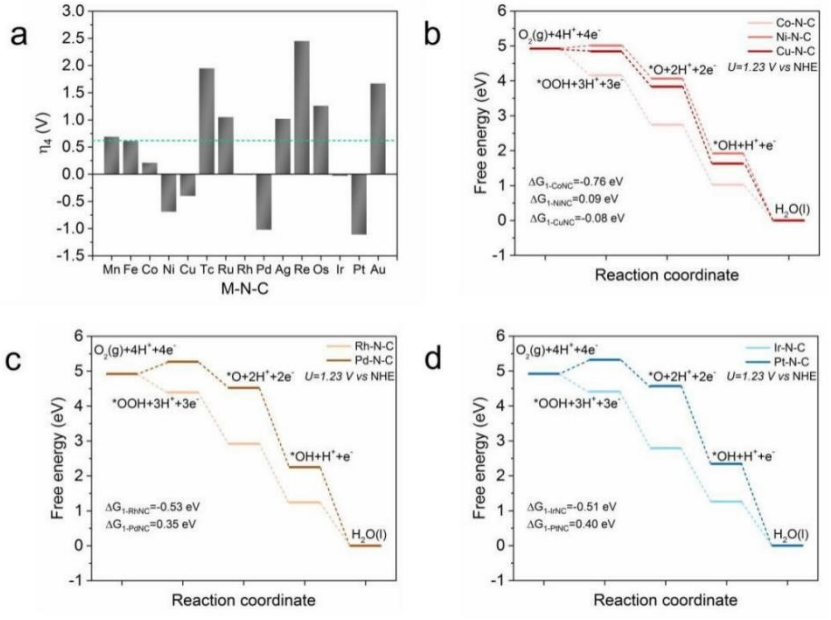

Figure S 2. (a) The overpotential of step $*OH+H^++e^-\rightarrow H_2O(l)$ for M-N-C. The ORR free energy diagram of (b) Co/Ni/Cu-N-C, (c) Rh/Pd-N-C and (d) Ir/Pt-N-C.

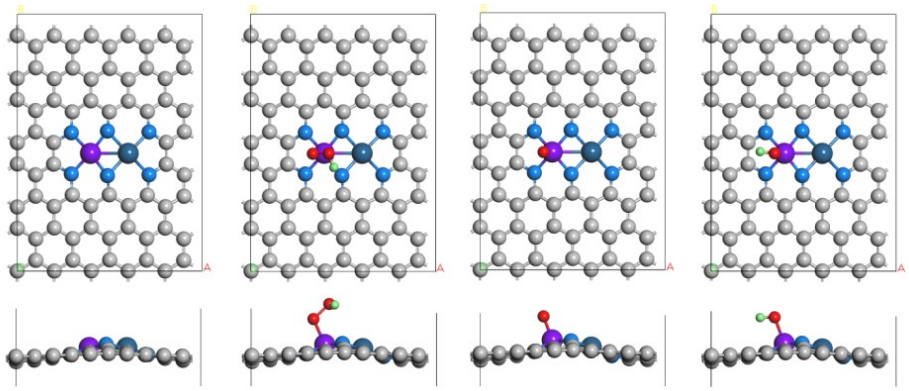

Figure S 3. The optimized structures FePt-N-C, *OOH-FePt-N-C, *O-FePt-N-C and *OH-FePt-N-C. Gray: C; Purple: Fe; Dark blue: Pt; Blue: N; Red: O; Green: H.

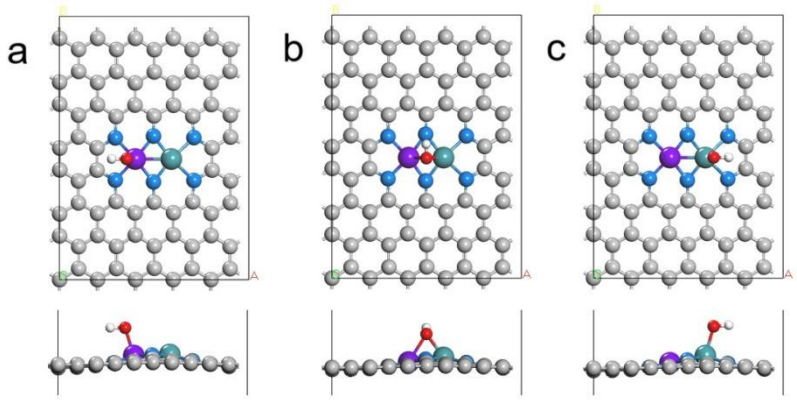

Figure S 4. The optimised adsorption structures of OH on Fe, M and the bridge site

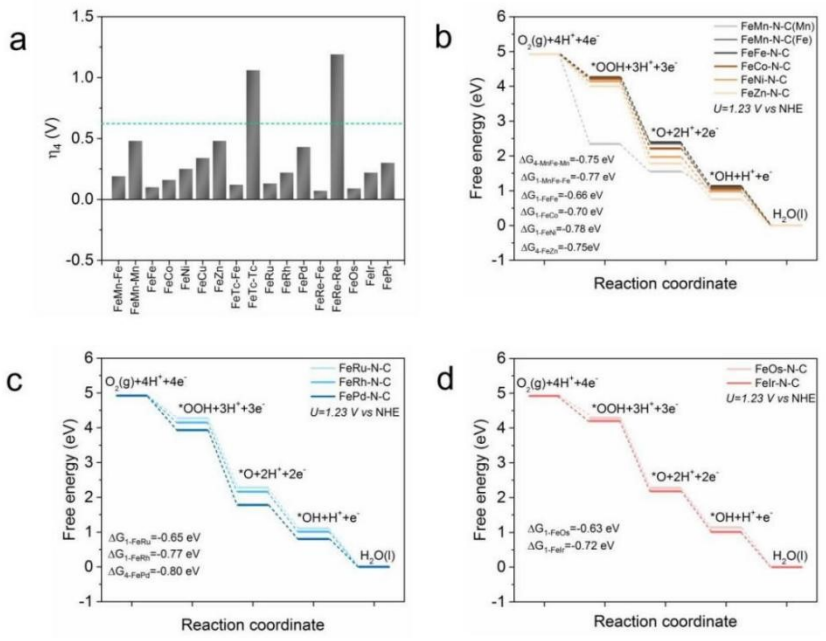

Figure S 5. (a) The overpotential of step *OH+H$^+$+e$^-$→H_2O(l) for FeM-N-C. The ORR free energy diagram of (b) FeM-N-C (M=Mn, Fe, Co, Ni, Zn), (c) FeM-N-C (M=Ru, Rh, Pd) and (d) FeM-N-C (M=Os, Ir).

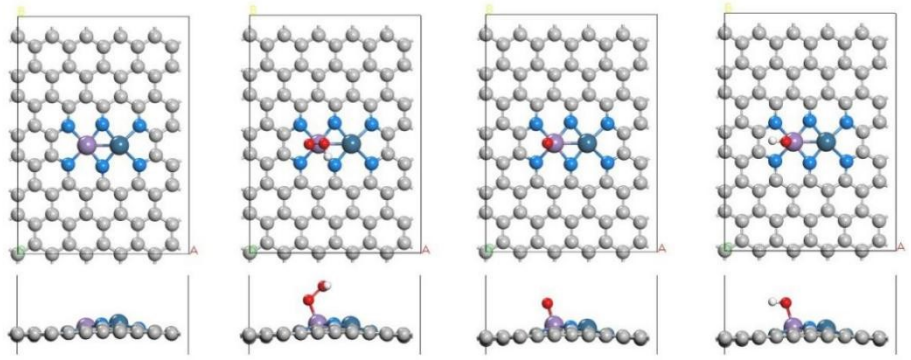

Figure S 6. The optimized structures MnCo-N-C, *OOH-MnCo-N-C, *O-MnCo-N-C and *OH-MnCo-N-C. Gray: C; Purple: Mn; Cyan: Co; Blue: N; Red: O; White: H.

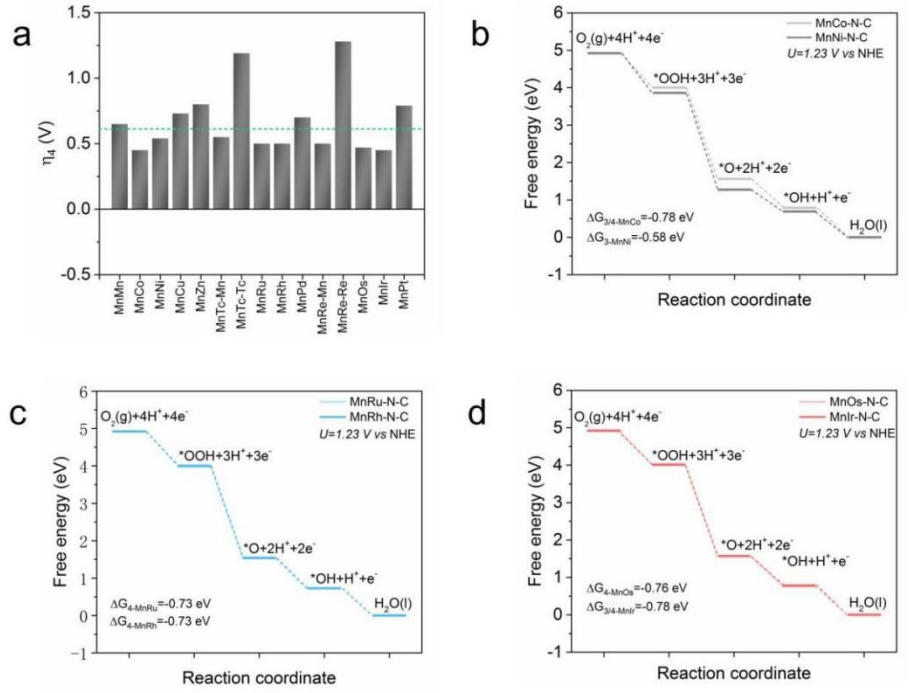

Figure S 7. (a) The overpotential of step *OH+H$^+$+e$^-$→H_2O(l) for MnM-N-C. The ORR free energy diagram of (b) MnM-N-C (M=Co, Ni), (c) MnM-N-C (M=Ru, Rh) and (d) MnM-N-C (M=Os, Ir).

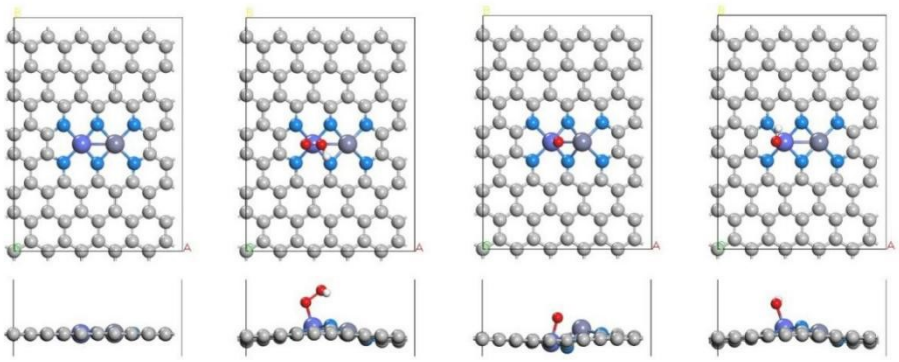

Figure S 8. The optimized structures Fe-N-C, *OOH-Fe-N-C, *O-Fe-N-C and *OH-Fe-N-C. Gray: C; Purple: Fe; Blue: N; Red: O; Green: H.

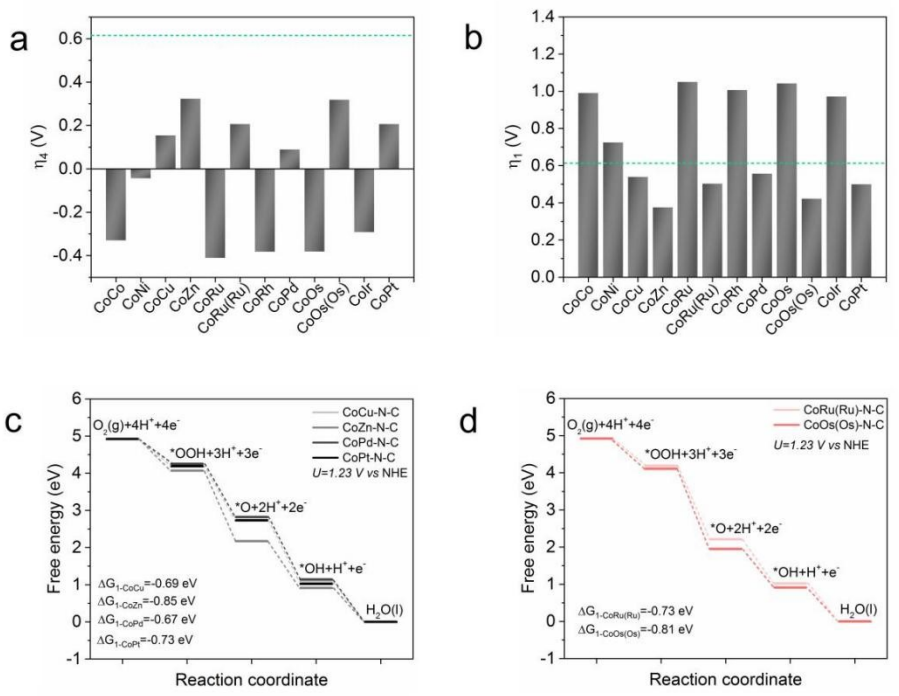

Figure S 9. The overpotential of (a) step *OH+H$^+$+e$^-$→H$_2$O(l) and (b)step O$_2$(g)+H$^+$+e$^-$→*OOH for CoM-N-C. The ORR free energy diagram of (c) CoM-N-C (M=Co, Zn, Pd, Pt), and (d) CoM-N-C (M=Ru, Os).

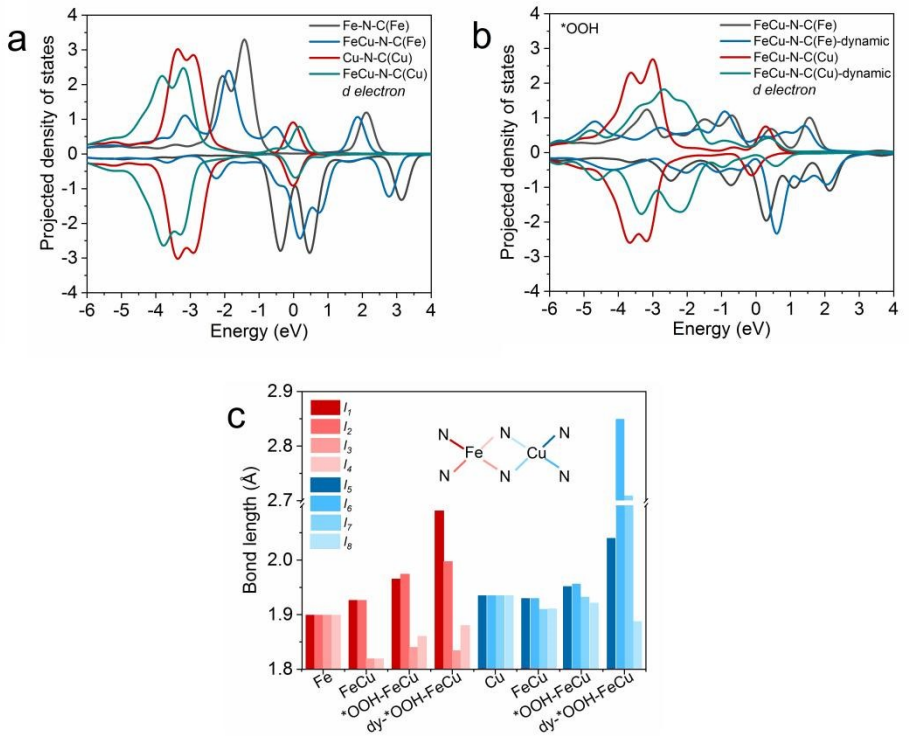

Figure S 10. The overpotential of (a) step $*OH+H^{+}+e^{-}\rightarrow H_2O(l)$ and (b)step $O_2(g)+H^{+}+e^{-}\rightarrow *OOH$ for CoM-N-C. The ORR free energy diagram of (c) CoM-N-C (M=Co, Zn, Pd, Pt), and (d) CoM-N-C (M=Ru, Os).

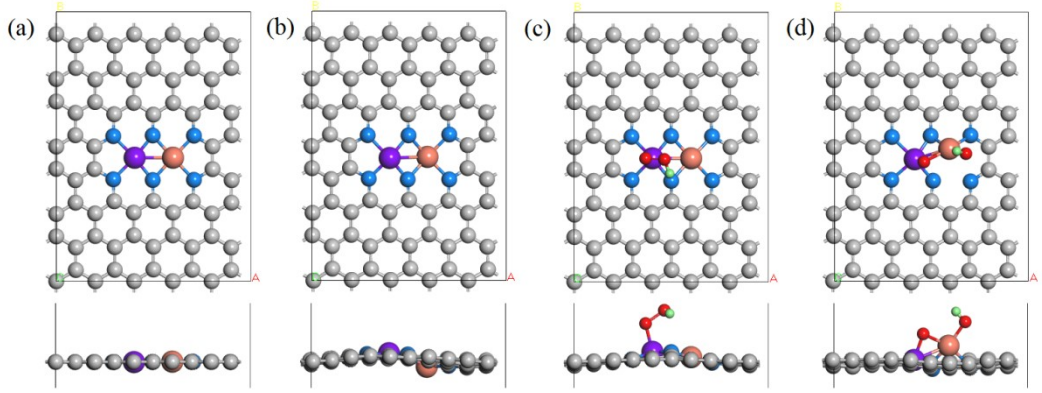

Figure S 11. The initial (a, c) and dynamic structure (b, d) of FeCu-N-C and *OOH-FeCu-N-C, respectively.

Table S 1 The zero point energies and entropic corrections of oxygenates at 298.15 K

Species	ZPE(*1*)	TS(*1*)	ZPE(*2*)	TS(*2*)	ZPE(*3*)	TS(*3*)	ZPE*	TS*
O*	0.05	0	0.084	0.05	0.05	0.05	0.09	0.05
OH*	0.36	0.06	0.386	0.07	0.37	0.1	0.36	0.10
OOH*	0.4	0.08	0.457	0.16	0.46	0.16	0.45	0.17
O_2	0.11	0.64	-	-	-	-	-	-
H_2	0.27	0.41	0.27	0.41	0.27	0.41	0.27	0.41
H_2O	0.56	0.67	0.56	0.67	0.56	0.67	0.56	0.67

*The present work.

Table S2 The ORR activity of M-N-C SACs

M-N-C	ΔG_{OH} (eV)	η_4 (V)	ΔG_{OOH} (eV)	η_1 (V)	ΔG_O (eV)	η_2 (V)	η_3 (V)
Mn	0.54	0.69					
Fe	0.62	0.61	3.77	0.08	1.41	-1.13	0.44
Co	1.02	0.21	4.16	0.47	2.74	-0.18	-0.49
Ni	1.92	-0.69	5.01	1.32			
Cu	1.63	-0.40	4.84	1.15			
Zn	0.57	0.66					
Tc	-0.72	1.95					
Ru	0.18	1.05					
Rh	1.24	-0.01	4.39	0.70			
Pd	2.25	-1.02	5.27	1.58			
Ag	0.21	1.02					
Cd	-1.13	2.36					
Re	-1.22	2.45					
Os	-0.03	1.26					
Ir	1.26	-0.03	4.41	0.72			
Pt	2.34	-1.11	5.32	1.63			
Au	-0.44	1.67					
Hg	-2.31	3.54					

Table S3 The formation energy of FeM-N-C DACs and M-N-C SACs

	$\Delta E_f(M_1M_2N_6)$	$\Delta E_f(M_1N_4)+\Delta E_f(M_2N_4)$
FeMn	-7.48	-6.16
FeFe	-7.98	-7.18
FeCo	-7.89	-7.37
FeNi	-6.92	-7.03
FeCu	-4.24	-4.62
FeZn	-2.56	-3.41
FeTc	-8.11	-5.70

FeRu	-7.96	-6.20
FeRh	-6.66	-6.01
FePd	-3.54	-3.83
FeRe	-7.63	-4.87
FeOs	-7.25	-5.26
FeIr	-5.50	-4.80
FePt	-2.24	-2.46

Table S4 The adsorption energy of OH on different sites of M_1M_2-N-C DACs

	Mn site	M site	Bridge site
MnMn-N-C	0.29	-	Mn site
MnCo-N-C	0.49	1.38	Mn site
MnNi-N-C	0.40	1.63	Mn site
MnCu-N-C	0.22	1.39	Mn site
MnZn-N-C	0.14	-0.06	0.37
MnTc-N-C	0.39	-0.25	Tc site
MnRu-N-C	0.44	0.72	Ru site
MnRh-N-C	0.44	1.44	Mn site
MnPd-N-C	0.24	1.81	Mn site
MnRe-N-C	0.44	-0.34	Re site
MnOs-N-C	0.48	0.69	Mn site
MnIr-N-C	0.49	1.59	Mn site
MnPt-N-C	0.15	1.60	Mn site
	Fe site	M site	Bridge site
FeMn-N-C	0.75	0.46	Mn site
FeFe-N-C	0.84	-	Fe site
FeCo-N-C	0.78	1.32	Fe site
FeNi-N-C	0.69	1.67	Fe site
FeCu-N-C	0.60	1.47	Fe site
FeZn-N-C	0.44	0.13	0.19
FeTc-N-C	0.82	-0.11	Tc site
FeRu-N-C	0.81	0.71	Ru site
FeRh-N-C	0.72	1.50	Fe site
FePd-N-C	0.51	1.80	Fe site
FeRe-N-C	0.87	-0.25	Re site
FeOs-N-C	0.85	0.74	Os site
FeIr-N-C	0.72	1.39	Fe site
FePt-N-C	0.64	1.85	Fe site

	Co site	M site	Bridge site
CoCo-N-C	1.27	-	Co site
CoNi-N-C	0.98	1.68	Co site
CoCu-N-C	0.79	1.54	Co site
CoZn-N-C	0.62	0.21	0.43
CoRu-N-C	1.35	0.73	Ru site
CoRh-N-C	1.32	1.52	Co site
CoPd-N-C	0.85	1.77	Co site
CoOs-N-C	1.32	0.62	Os site
CoIr-N-C	1.23	1.41	Co site
CoPt-N-C	0.73	1.64	Co site

Table S5 The geometric and electronic property of FeM-N-C DACs

TM-N-C	Charge (Fe)	Spin (Fe)	l_{Fe-N}	l_{Fe-TM}
Fe	0.536	2.042	1.899*4	-
FeMn	0.439	0.670	1.808*2 1.939*2	2.261
FeFe	0498	1.144	1.799*2 1.953*2	2.238
FeCo	0.562	1.570	1.798*2 1.952*2	2.280
FeNi	0.551	1.940	1.807*2 1.931*2	2.409
FeCu	0.538	2.114	1.819*2 1.926*2	2.432
FeZn	0.499	2.038	1.825*2 1.918*2	2.436
$FeTc^{OH}$	0.484	1.446	1.863*2 1.936*2	2.352
FeRu	0.525	1.525	1.852*2 1.931*2	2.297
FeRh	0.486	1.581	1.827*2 1.931*2	2.326
FePd	0.563	1.846	1.822*2 1.915*2	2.430
$FeRe^{OH}$	0.472	1.439	1.877*2 1.935*2	2.379
FeOs	0.517	1.536	1.877*2 1.935*2	2.333
FeIr	0.573	1.630	1.858*2 1.940*2	2.369
FePt	0.605	2.020	1.875*2	2.510

			1.930*2	

References

1. S. Zhou, N. S. Liu, Z. Y. Wang, J. J. Zhao, Nitrogen-Doped Graphene on Transition Metal Substrates as Efficient Bifunctional Catalysts for Oxygen Reduction and Oxygen Evolution Reactions. *Acs Applied Materials & Interfaces* **9**, 22578-22587 (2017).
2. L. Yu, X. L. Pan, X. M. Cao, P. Hu, X. H. Bao, Oxygen reduction reaction mechanism on nitrogen-doped graphene: A density functional theory study. *Journal of Catalysis* **282**, 183-190 (2011).
3. X. M. Zhang *et al.*, Theoretical study of the strain effect on the oxygen reduction reaction activity and stability of FeNC catalyst. *New Journal of Chemistry* **44**, 6818-6824 (2020).